LAWRENCE
LIVERMORE
NATIONAL
LABORATORY

LLNL-CONF-485360

Advanced Lasers Systems for Mega Ray based Nuclear Materials Detection and Assay

D. Gibson, C. Ebbers, F. Albert, A. Bayramian, S. Betts, F. Hartemann, R. Marsh, M. Messerly, H. Phan, S. Wu, C. Siders, C. Barty

June 2, 2011

Insitute of Nuclear Materials Annual Meeting
Palm Desert, CA, United States
July 17, 2011 through July 21, 2011

Disclaimer

Advanced Laser Systems for MEGa-ray-based Nuclear Materials Detection and Assay

D. J. Gibson*, C. A. Ebbers*, F. Albert*, A. Bayramian*, S. M. Betts*, F. V. Hartemann*, R. A. Marsh*, M. J. Messerly*, H. H. Phan*, S. Wu*, C. W. Siders* and C. P. J. Barty*

*Lawrence Livermore National Laboratory, Livermore, CA 94550

Abstract. A Compton-scattering based, tunable MonoEnergetic Gamma-ray (MEGa-ray) source suitable for nuclear resonance fluorescence measurements requires specific performance parameters for the affiliated laser systems. Optimization of the number of photons/eV/s dictates a trade-off between shorter laser pulses to maximize the photon density, and narrower laser bandwidths to minimize the gamma-ray energy spread. Also required is a high-brightness electron beam, which in turn requires a second laser system, converted to UV, with a fast rise-time, long duration, and flat transverse profile. Furthermore, these lasers must be synchronized with each other and with the RF providing the electron bunch acceleration. Presented here is an overview of the laser system designed for LLNL's MEGa-ray source. This chirped-pulse-amplification (CPA)-based laser system starts with a fiber-based oscillator with is then split into two amplification chains. The first amplification chain produces 120 Hz, 1 mJ, 250 fs, 1053 nm laser pulses in a series of fiber amplifiers. This pulse is then frequency-quadupled to the UV, shaped spatially and stacked temporally to produce the desired laser distribution for the photocathode. The second amp chain generates a 120 Hz, 1 J, 10 ps, 1064 nm laser pulse using a combination of fiber amps and diode-pumped Nd:YAG heads. A novel hyper-dispersion stretcher/compressor pair allows CPA to work effectively with the narrow bandwidth of the gain medium. Finally, in order to increase the laser-to-gamma-ray conversion efficiency, the laser photons can be recirculated through the interaction point via an optical cavity that traps pulses using a frequency conversion process (a scheme known as "RING": Recirculation Injection via Nonlinear Gating).

INTRODUCTION

Tunable, narrow-bandwidth γ-ray sources have the potential to revolutionize nuclear physics in much the same way that lasers revolutionized atomic physics, allowing scientists to probe nuclei in a controlled manner over a broad range of energies. One of the more popular means to generate such a source is through the Compton scattering process: laser light scatters of a relativistic electron beam and the scattered photons carry off a fraction of the electron energy, emerging as γ-rays. Several sources relying on this technique have been demonstrated and used for nuclear experiments[1, 2, 3, 4], but all have relied on adapting a system designed for other purposes to accomdate the Compton scattering process.

At Livermore, a Mono-energetic Gamma-ray (MEGa-ray) source is under construction that has been designed from the ground up to optimize the gamma-ray parameters. This system is based on 11.424 GHz rf accelerator technology generating a 250 MeV beam, with a 532 nm laser scattering to produce ~ 2 MeV γ-rays[5]. Previous experience[6, 7] has demonstrated the feasibility of a Compton-scattering source for nuclear resonance fluorescence (NRF) measurements, a process which can provide isotope-specific identification of material[8], and the system currently being built has been designed to optimize performance for this process. NRF lines are generally found in

the $0.5-3$ MeV energy range, and have bandwidths on the order of 10^{-6} ($\sim$ 1 eV). Therefore, in designing a source, it is important to maximize the photon flux in the resonant bandwidth (photons/s/eV) while minimizing the number of photons outside that bandwidth, which can only contribute noise to the experimental measurement. A source bandwidth of 0.2% is a desirable goal.

The energy of the scattered electron beam in a head-on collision is given by

$$E_\gamma = \frac{4\gamma^2}{1+\gamma^2\theta^2+4\gamma\frac{\lambda}{\lambda_c}}E_l \tag{1}$$

where λ is the laser wavelength, $E_l = \frac{hc}{\lambda}$ is the energy of the laser photon, γ is the electron Lorentz factor, $\lambda_c = \frac{h}{mc} = 2.426\times10^{-12}$ m is the Compton wavelength, and θ is the observation angle relative to the electron direction. This equation shows that, to minimize the bandwidth, the laser bandwidth, electron energy spread, and electron beam emittance must all be minimized. These requirements drive the design parameters of the laser systems used for the source.

PHOTOINJECTION DRIVE LASER

The energy spread of the electrons is driven mostly by the variation in accelerating gradient during the length of the bunch. With an 11.424 GHz accelerating field, this means the bunch length must be keep at 2 ps or shorter to keep the energy spread in the 0.2% range. To generate a high-charge, short bunch, we are using an X-band photoinjector[9] which requires a driving laser. To minimize the emittance of the electron beam at the output of the gun, it's important that this beam has a fast rise and fall time and a uniform transverse profile, which requires shaping of the laser pulse.

Pulse Amplification

Both the Photoinjection Drive Laser (PDL) and the Interaction Laser System (ILS) start with the same fiber oscillator. This oscillator produces 250 pJ, sub 100 fs, near transform limited pulses at a 40.8 MHz repetition rate with a full bandwidth from 1035 nm to 1068 nm. A 20 nm bandwidth portion of the full spectrum centered at 1053 nm seeds the PDL; a 1 nm portion bandwidth centered at 1064 nm seeds the ILS (Fig. 1).

To avoid damage and nonlinear effects in the amplifying medium, chirped-pulse amplification is used. The sub-ps pulse from the oscillator is sent through an Offner pulse stretcher which imparts a transmission delay that is a function of wavelength, resulting in a pulse that is $\sim$3 ns long with a commensurately lower peak intensity. The stretcher output is then coupled back into a fiber with a 10% total transmission efficiency, as shown in Fig. 1.

A series of 5 telecom-type preamplifiers increase the pulse energy to 1 μJ at 10 kHz. Next, two bulk/hybrid 41 μm core photonic crystal fiber amps boost the pulse energy to 100 μJ. An 85 μm core photonic crystal rod amplifier provides the final 10 dB of gain, resulting in a final energy of 1 mJ, that should be compressable to a 214 fs FWHM pulse.

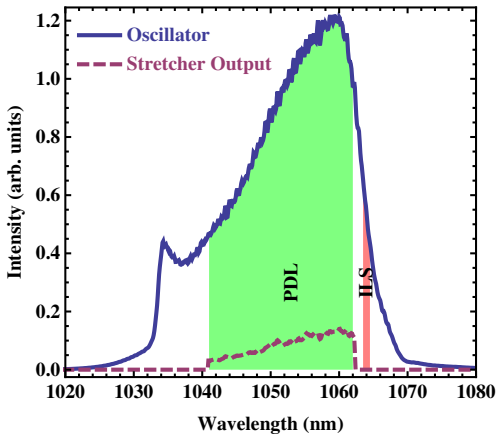

FIGURE 1. Spectrum of oscillator and stretcher outputs, showing the bandwidths used for the PDL and ILS lasers.

Pulse Shaping

The amplified pulse is frequency converted to the fourth harmonic, 261 nm, to overcome the work function of the Cu photocathode. This pulse is then shaped in space and time to generate the uniform cylindrical distribution, necessary to minimize electron bunch emittance, to illuminate the cathode.

Temporal shaping is provided by a hyper-Michelson pulse stacker[10], in which a series of beamsplitters multiplies a single input pulse into 8 copies with a precisely controllable spacing. This allows the 250 fs input pulse to be converted into a 2 ps long pulse with a $<$200 fs rise time. Using a waveplate and polarizer to recombine the pulses at the end of the beamsplitter chain means no light is wasted, and efficiency is limited only by the quality of the UV mirrors.

Spatial shaping is accomplished with a refractive beam shaper, which redistributes light from the center of the input gaussian distribution towards the outer edge (Fig. 2). Transmission efficiency through the refractive shaper was measured at 70%. A previous scheme, where a small aperture was used to clip all but the centermost portion of the beam, also produced a beam sufficient for cathode illumination. This method was much simpler to implement, but wasted 88% of the incoming laser pulse and so is very inefficient. Simulations of an electron beam in PARMELA, with an initial spatial distribution matching that measured using the refractive shaper, showed an emittance at the end of the first section similar to that for a flat distribution (Fig. 2, bottom). The asymmetry observed in the emittance is attributable to the asymmetry in the initial gaussian profile, shown in Fig. 2, top.

INTERACTION LASER SYSTEM

To minimize the bandwidth of the γ-ray source, it's important that the bandwidth of the interaction laser be minimized. However, the interaction geometry must be kept in mind; the laser will be focused to interact with the electron beam. At distances z from the focal plane of the laser, the $1/e^2$ intensity radius w of the beam increases according to

$$w(z) = w_0\sqrt{1+\left(\frac{z}{z_r}\right)^2} \qquad z_r = \frac{\pi w_0^2}{\lambda} \tag{2}$$

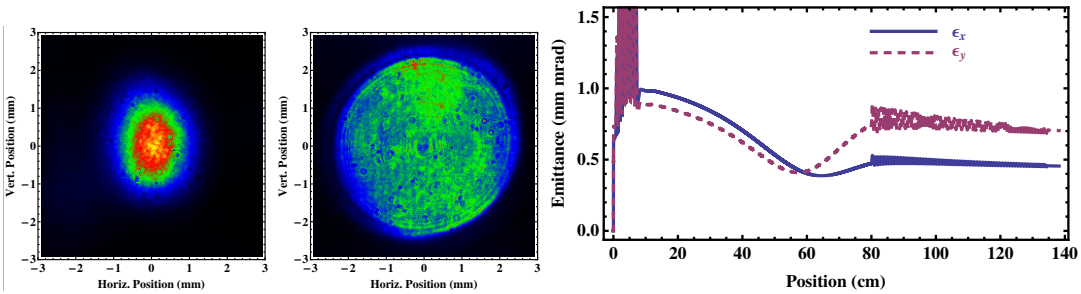

FIGURE 2. Top: Profiles before and after refractive beam shaper. Left: before, Right: after. Bottom: Simulated emittance growth of electron beam through X-band gun and first accelerating section with starting distribution shown above

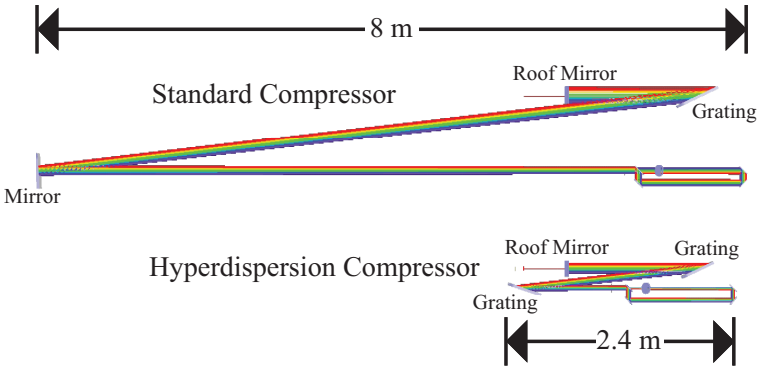

FIGURE 3. Comparison of the size of a standard (top) and hyperdispersion (bottom) compressor with a dispersion of 6650 ps/nm.

where $w_0 = w(0)$ corresponds to the laser focal size and z_r is known as the Rayleigh range. This increase in beam size causes the photon density (and therefore the scattering rate) to drop. For $w_0 = 40$ μm and $\lambda = 532$ nm, z_r corresponds to an optimal interaction length of ~ 30 ps. Having a pulse longer than this means part of the interaction will occur away from the focus, so more laser energy per scattered photon would be required. Since the pulse length and the bandwidth of a laser pulse are inversely related, this $\sim$10 ps requirement limits how narrow the bandwidth can be.

Hyperdispersion

Nd:YAG turns out to be an ideal material for building the amplifier needed for the ILS, since it has been used for decades to produce Joule-level pulses of a few ns in length and has bandwidth sufficient to support a 10 ps pulse. However, stretching a 1 nm bandwidth pulse to 6 ns requires a much larger dispersion than a conventional stretcher and compressor can provide in a reasonable space. To create a dispersion of 6000 ps/nm, a conventional stretcher would require a grating separation of $\sim$ 30 m. By cascading two gratings in sequence, with matching incidence angles, the dispersion can be significantly increased, allowing a table-sized stretcher and compressor to successfully chirp a 1 nm bandwidth laser to a few ns in length. Fig. 3 shows a comparison of the size of two compressors with equivalent dispersion of 6650 ps/nm (4000 ps^2).This “hyperdispersion" pulse stretcher has been demonstrated[11] to compress a 1 J laser pulse to 8.3 ps (Fig. 4).

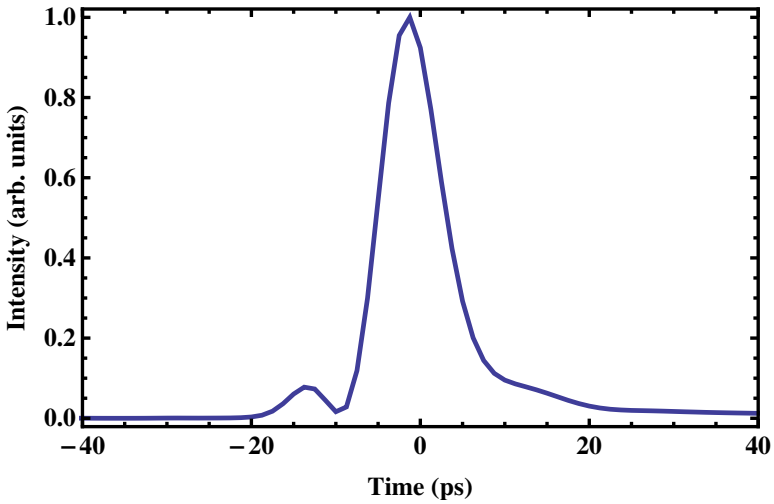

FIGURE 4. ILS pulse trace reconstructed from frequency resolved optical gating (FROG) pulse measurement showing 8.3 ps FHWM pulse length.

Amplification

The stretched pulse is first amplified up to $\sim$ 100 μJ in a fiber front end that matches the first stages of the PDL amplifier. It is then sent into a bulk amplifier. The kW-class diode pumped amplifier consists of two heads (Northrop Grumman, REA series), each containing a 1 cm diameter, 14.6 cm long Nd:YAG rod. A gaussian to flattop refractive shaper modifies the seed beam profile to optimally fill the amplifier rods, maximizing extraction efficiency and minimizing diffractive losses. The seed beam four-passes the first amplifier head and double passes the second head producing 1 J prior to compression, similar to other high average power lasers[13]. A deformable mirror compensates for thermal lensing and low-order aberrations in the amplifier. The beam is relay imaged throughout the system to maintain beam quality and compensate for thermal birefringence. To produce higher energy γ-rays, we will frequency double the output pulse and generate $\sim$200 mJ at 532 nm.

PULSE RECIRCULATION

The MEGa-ray source design includes an option for laser pulse recirculation. Because Compton scattering is a low efficiency process, only 1 in 10^{10} of the incident laser photons is used up in the interaction. Reusing laser photons would both, improve the conversion efficiency, and increase the generated γ-ray flux. High power, high energy, short pulse recirculation is very challenging, however. Recently, we successfully demonstrated a scheme, termed Recirculation Injection by Nonlinear Gating (RING), designed for our laser system [12].

In the simplest implementation of this technique, shown in Fig. 5, the incident laser pulse at the fundamental frequency enters the resonator and is efficiently frequency doubled. The resonator mirrors are dichroic, coated to transmit the 1ω light and reflect at 2ω. The upconverted 2ω pulse then becomes trapped inside the cavity. After several hundred roundtrips, the laser pulse decays primarily due to Fresnel losses at the crystal faces and cavity mirrors. Compared to active (electro-

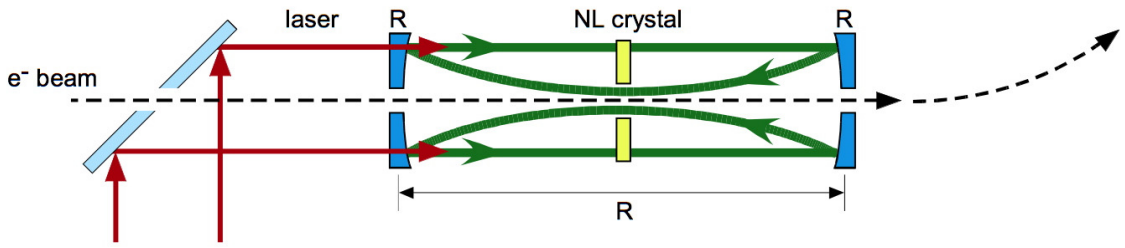

FIGURE 5. One possible configuration for recirculating a laser pulse at a Compton interaction point.

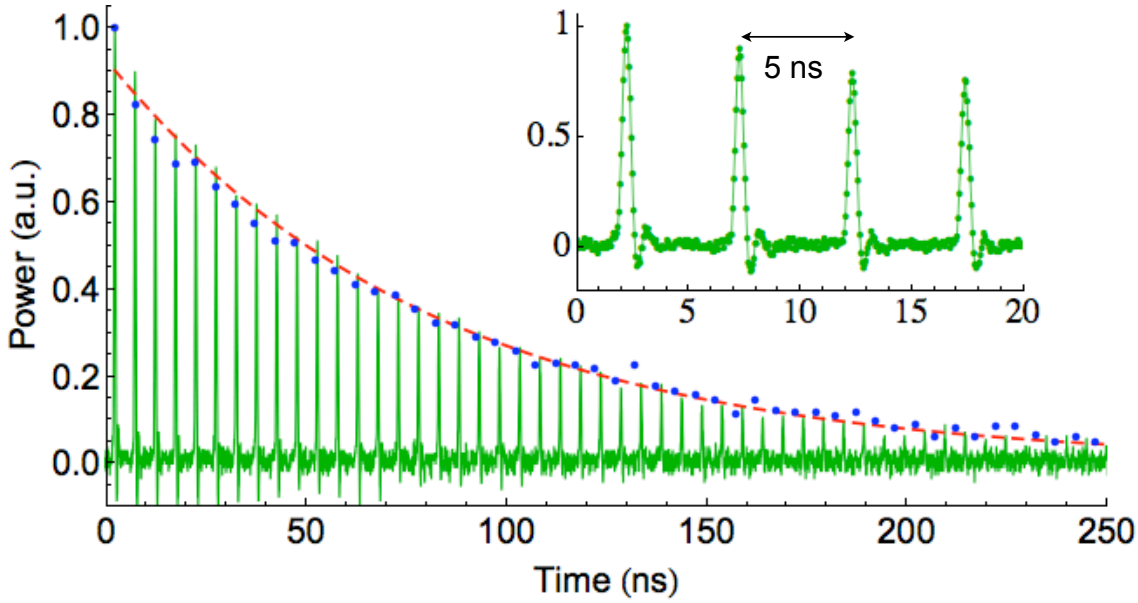

FIGURE 6. Recirculating laser power measurement showing a 14x increase in integrated laser flux to the interaction point with a trapped 200 mJ, 10 ps laser pulse.

optic or accousto-optic) pulse switching, the pulse in RING scheme traverses a significantly thinner optical material, reducing nonlinear phase accumulation. Nonlinear phase accumulation limits the total number of roundtrips, because it causes beam and pulse break-up.

In an off-line demonstration, we achieved 14x average power enhancement of a 200 mJ, 10 ps pulse (Fig. 6). By improving the spatial beam quality of the incident pulse, we expect to achieve over 30x average power enhancement, equalling our low energy (500 μJ) results obtained with a different laser system.

RING operates in a burst-pulse, multi-bunch mode, where the laser repetition frequency sets the spacing between the macro-bunches, and the cavity roundtrip time ($\approx$10 ns) determines the micro-pulse spacing within the macro-bunch. The pulse format of the photogun laser needs to match this burst mode to realize RING enhancement of the γ-ray flux. Studies of the effects of micro-bunch electron structure on beam emittance are currently under way.

CONCLUSIONS

We have discussed the design of the laser systems associated with the MEGa-ray project at LLNL. Choosing the ultimate application of the MEGa-ray source currently under construction to be nuclear resonance fluorescence measurements leads to the requirement of minimal γ-ray bandwidth. This in turn leads to requirements of narrow bandwidth on the interaction laser, which requires a novel hyperdispersion pulse stretcher and compressor. With this hyperdispersion technology in hand, commercial Nd:YAG heads become the ideal amplfier for the interaction laser. Also required is a drive laser for the X-band photoinjector that provides a uniformly filled cylinder of photons, requiring shaping of the laser beam in both time, using a hyper-Michelson pulse stacker, and in space, using a refractive beam shaper. The fast rise times required necessitate careful design of the CPA hardware to allow recompression of the fiber-amplified laser pulse to the 250 fs range. It is expected that the system designed at LLNL can meet all these requirements and generate a γ-ray beam with minimal bandwidth. This work performed under the auspices of the U.S. Department of Energy by Lawrence Livermore National Laboratory under Contract DE-AC52-07NA27344.

REFERENCES

1. H. R. Weller, M. W. Ahmed, H. Gao, W. Tornow, Y. K. Wu, M. Gai, and R. Miskimen, *Prog. Part. and Nuc. Phys.* **62**, 257 – 303 (2009).
2. E. C. Schreiber, R. S. Canon, B. T. Crowley, C. R. Howell, J. H. Kelley, V. N. Litvinenko, S. O. Nelson, S. H. Park, I. V. Pinayev, R. M. Prior, K. Sabourov, M. Spraker, W. Tornow, Y. Wu, E. A. Wulf, and H. R. Weller, *Phys. Rev. C* **61**, 061604 (2000).
3. C. Thorn, G. Giordano, O. Kistner, G. Matone, A. Sandorfi, C. Schaerf, and C. Whisnant, *Nuc. Inst. Meth. Phys. Res. A* **285**, 447 – 458 (1989), ISSN 0168-9002.
4. O. Bartalini, V. Bellini, J. P. Bocquet, M. Capogni, L. Casano, M. Castoldi, P. Calvat, A. D'Angelo, R. D. Salvo, A. Fantini, C. Gaulard, G. Gervino, F. Ghio, B. Girolami, A. Giusa, V. Kouznetsov, A. Lapik, P. L. Sandri, A. Lleres, D. Moricciani, A. N. Mushkarenkov, V. Nedorezov, L. Nicoletti, C. Perrin, D. Rebreyend, F. Renard, N. Rudnev, T. Russew, G. Russo, C. Schaerf, M. L. Sperduto, M. C. Sutera, and A. Turinge, *Eur. Phys J. A* **26**, 399–419 (2005).
5. F. V. Hartemann, "Overview of Current Progress on the LLNL Center for Nuclear Photonics and Mono-energetic Gamma-ray Source," in *Proceedings of the 2011 Particle Accelerator Conference*, THP182 (2011).
6. D. J. Gibson, F. Albert, S. G. Anderson, S. M. Betts, M. J. Messerly, H. H. Phan, V. A. Semenov, M. Y. Shverdin, A. M. Tremaine, F. V. Hartemann, C. W. Siders, D. P. McNabb, and C. P. J. Barty, *Phys. Rev. ST Accel. Beams* **13**, 070703 (2010).
7. F. Albert, S. G. Anderson, D. J. Gibson, C. A. Hagmann, M. S. Johnson, M. Messerly, V. Semenov, M. Y. Shverdin, B. Rusnak, A. M. Tremaine, F. V. Hartemann, C. W. Siders, D. P. McNabb, and C. P. J. Barty, *Phys. Rev. ST Accel. Beams* **13**, 070704 (2010).
8. J. Pruet, D. P. McNabb, C. A. Hagmann, F. V. Hartemann, and C. P. J. Barty, *J. App. Phys.* **99**, 123102 (2006).
9. R. Marsh, "X-Band RF Photoinjector Research and Development," in *Proceedings of the 2011 Particle Accelerator Conference*, TUP023 (2011).
10. C. W. Siders, J. L. W. Siders, A. J. Taylor, S.-G. Park, and A. M. Weiner, *Appl. Opt.* **37**, 5302–5305 (1998).
11. M. Y. Shverdin, F. Albert, S. G. Anderson, S. M. Betts, D. J. Gibson, M. J. Messerly, F. V. Hartemann, C. W. Siders, and C. P. J. Barty, *Opt. Lett.* **35**, 2478–2480 (2010).
12. M. Y. Shverdin, I. Jovanovic, V. A. Semenov, S. M. Betts, C. Brown, D. J.Gibson, R. M. Shuttlesworth, F. V. Hartemann, C. W. Siders, C. P. J. Barty, *Opt. Lett.* **35**, 2224–2226 (2010).
13. A. Bayramian, P. Armstrong, E. Ault, R. Beach, C. Bibeau, J. Caird, R. Campbell, B. Chai, J. Dawson, C. Ebbers, A. Erlandson, Y. Fei, B. Freitas, R. Kent, Z. Liao, T. Ladran, J. Menapace, B. Molander, S. Payne, N. Peterson, M. Randles, K. Schaffers, S. Sutton, J. Tassano, S. Telford, and E Utterback, *Fus. Sci. Tech.*, **52**, 383–387, (2007).